Chirality in $(\vec{p}, 2p)$ reaction and helicity dependence of the cross section

T. Edagawa[1], K. Yoshida[1,2*] , S. Kawase[3], K. Ogata[4,1] and M. Sasano[5]
[1] *Research Center for Nuclear Physics, Osaka University, Ibaraki 567-0047, Japan*
[2] *Interdisciplinary Theoretical and Mathematical Sciences Program (iTHEMS), RIKEN, Wako 351-0198, Japan*
[3] *Department of Advanced Energy Science and Engineering, Kyushu University, Kasuga, Fukuoka 816-8580, Japan*
[4] *Department of Physics, Kyushu University, Fukuoka 819-0395, Japan*
[5] *RIKEN Nishina Center, Hirosawa 2-1, Wako, Saitama 351-0198, Japan*

1 Introduction

We present a concise summary of our study of chirality induced in intermediate-energy proton knockout reactions by longitudinal proton polarization [1]. The primary reaction of interest is $^{16}\mathrm{O}(\vec{p}, 2p)^{15}\mathrm{N}$ at 250 MeV. The central claim is that beam helicity can be transferred to a measurable chirality in the non-coplanar final-state momenta.

In the laboratory frame, mirror symmetry of isolated nuclei implies that chiral preference does not appear unless an external probe breaks the symmetry. A longitudinally polarized proton beam provides that probe. In quasi-free kinematics, strong spin correlation in the elementary NN process selects the spin orientation of the struck nucleon. These features are understood as the origins of the so-called Maris effect [2–8]. When combined with single-particle orbital motion and nuclear distortion, this produces a helicity-dependent asymmetry in the final state.

2 Vector analyzing power and an intuitive picture

Here, a set of momenta in the final state is denoted by $\mathcal{K} = (\boldsymbol{K}_1, \boldsymbol{K}_2, \boldsymbol{K}_\mathrm{B})$, where the labels 0, 1, 2, and B denote the initial proton, the scattered proton, the knocked-out proton and the residual nucleus, respectively. The $(\vec{p}, 2p)$ cross section with positive (+) and negative (−) helicity can be expressed as a function of $\mathcal{K}$ as $\sigma_\pm(\mathcal{K})$. We denote the mirror partner of $\mathcal{K}$ under $x \to -x$ as $\tilde{\mathcal{K}}$.

The vector analyzing power along the z-axis (beam direction, equivalent to the helicity) is defined by

$$A_z = p_z \frac{\sigma_+(\mathcal{K}) - \sigma_+(\tilde{\mathcal{K}})}{\sigma_+(\mathcal{K}) + \sigma_+(\tilde{\mathcal{K}})}, \tag{1}$$

with p_z being the polarization of the beam particle. A_z can be defined equivalently by

$$A_z = p_z \frac{\sigma_+(\mathcal{K}) - \sigma_-(\mathcal{K})}{\sigma_+(\mathcal{K}) + \sigma_-(\mathcal{K})}. \tag{2}$$

Thus, A_z directly measures how beam helicity selects one chirality of final-state kinematics $\mathcal{K}$ over its mirror partner $\tilde{\mathcal{K}}$. The mechanism can be interpreted in three steps: (i) strong spin correlation in quasi-free NN scattering, (ii) spin-orbit coupling in bound single-particle states, and (iii) kinematical selection of the reaction region due to the distortion (absorption) of the optical potential. The readers are referred to Ref. [1] for the details of the framework.

We evaluate helicity-dependent cross sections for non-coplanar kinematics characterized by the relative azimuthal angle of the two protons in the final state, ϕ_{12}. When $\phi_{12} = 180°$, all the particles are in the same 2D plane (coplanar condition), and $A_z = 0$ from the symmetry. Thus, deviation from $\phi_{12} = 180°$ serves as a measure of chirality in the $(p, 2p)$ reaction.

Figure 1 shows a typical non-coplanar $(\vec{p}, 2p)$ kinematics. The proton beam with momentum (wave number) K_0 is incident on the target nucleus A. A typical kinematic configuration is shown in the left panel of Fig. 1. In the $(\vec{p}, 2p)$ kinematics, the vector $\boldsymbol{K}_0$ defines the z-axis. $\boldsymbol{K}_0$ and $\boldsymbol{K}_1$ are in the z-x plane, and the x-axis is defined so that the x component of $\boldsymbol{K}_1$ is positive. The y-axis is defined by $\boldsymbol{K}_0 \times \boldsymbol{K}_1$. Here, we define the "right side" as the $x < 0$ region, and the "left side" as the $x > 0$ region. Similarly, the $y > 0$ region is the "upper side" and $y < 0$ region is the "lower side". In a semi-classical understanding, if we select kinematics with small $\boldsymbol{K}_2$ directed to the right, this indicates that the proton is knocked out from the right side of the target nucleus, since the proton with low K_2 is emitted from the nucleus without being absorbed by the residue. Assuming a proton knockout reaction from the $p_{1/2}$ single-particle orbital, for example, the p-wave orbital angular momentum of

*Corresponding author

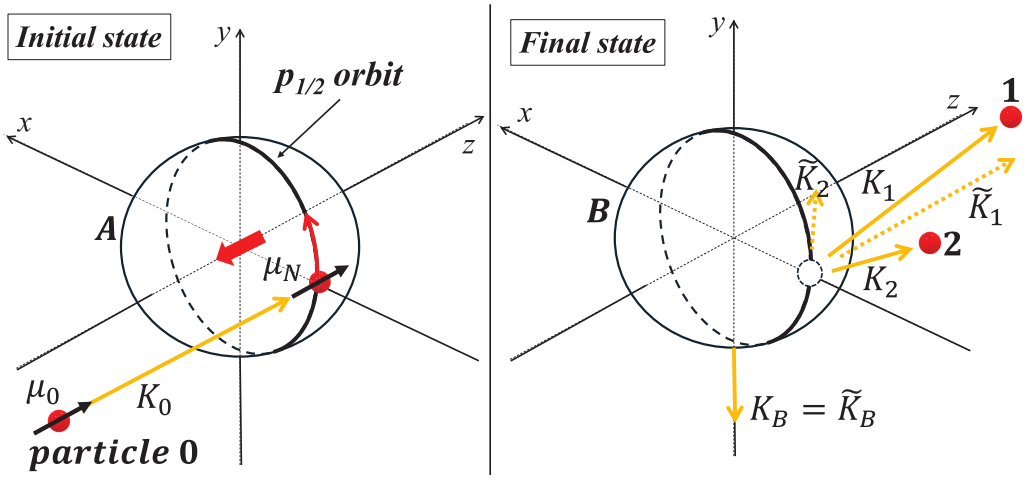

Figure 1: Schematic view of chirality generation in non-coplanar $^{16}\mathrm{O}(\vec{p}, pN)$ kinematics. The figure is taken from Ref. [1].

the struck proton and its spin are anti-aligned. There are two possible configurations of such classical motion. One is that the proton orbital angular momentum is antiparallel to the beam direction, and the spin direction of the struck proton is parallel to the beam, as shown in the left panel of Fig. 1, and vice versa. These two can be distinguished by the beam proton helicity. Since the pp scattering amplitude favors the spin-parallel pair ($C_{zz} \approx 1$) at this energy region, a configuration in which the helicity of the beam and the struck proton inside the target has the same spin direction, $\mu_0 = \mu_N$, dominates the $(\vec{p}, 2p)$ cross section. In such a case, the struck proton is likely knocked out to the upper side ($y > 0$), reflecting its orbital motion in the initial state. This leads to the conclusion that $A_z > 0$ for $(\vec{p}, 2p)$ from the $p_{1/2}$ orbital if $\phi_{12} < 180°$. A similar argument gives the behavior of A_z for $0p_{1/2}$ and $0p_{3/2}$ proton knockout around $\phi_{12} = 180°$ as shown in Table 1.

Table 1: The sign of A_z expected from semiclassical picture.

	$\phi_{12} < 180°$	$\phi_{12} = 180°$	$180° < \phi_{12}$
$A_z(0p_{1/2})$	+	0	−
$A_z(0p_{3/2})$	−	0	+

3 Theoretical framework and results

The quantitative analysis is performed based on the distorted-wave impulse approximation (DWIA) [4, 9–11]. The transition amplitude is constructed from distorted waves generated using optical potentials [12–14], an effective NN interaction in free space [15, 16], and the bound-state proton wave function [17]. Numerical calculations were performed using the PIKOE code [11]. See Ref. [1] for further details.

Figure 2 presents the theoretical results. The left panel shows the triple differential cross section (TDX) of $^{16}\mathrm{O}(\vec{p}, 2p)^{15}\mathrm{N}$ reaction from the $0p_{1/2}$ and the $0p_{3/2}$ orbitals, and the middle panel shows A_z of the same reactions. First, A_z vanishes at the coplanar point $\phi_{12} = 180°$, as required by symmetry. Second, mirror

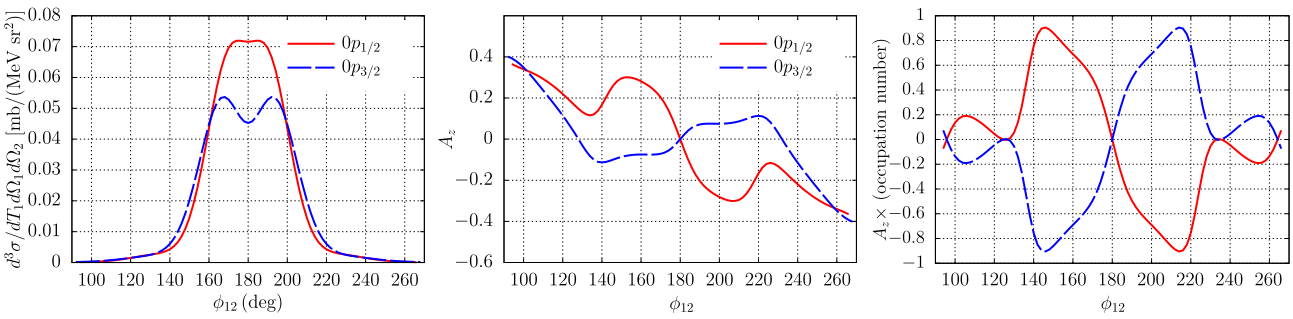

Figure 2: Calculated TDX (left) and A_z (middle) for $^{16}\mathrm{O}(\vec{p}, 2p)$ at 250 MeV as a function of ϕ_{12}. These figures are taken from Ref. [1]. The right panel shows A_z of a simplified DWIA calculation. See text for details.

transformation gives $A_z(\phi_{12}) = -A_z(360^\circ - \phi_{12})$. Third, proton knockout reactions from the $0p_{1/2}$ and $0p_{3/2}$ orbitals yield opposite signs of A_z, as expected from Table 1, showing opposite beam helicity dependence for the $(\vec{p}, 2p)$ reaction from the $0p_{1/2}$ and the $0p_{3/2}$ orbitals. Notably, both TDX and A_z are large in $140^\circ \lesssim \phi_{12} \lesssim 220^\circ$, making it suitable for experiments.

A simplified calculation can be obtained by neglecting several terms and inputs in the standard DWIA framework. The intuitive picture can be reproduced by neglecting 1) spin-orbit potential for both scattering and binding potentials for the initial and final protons, 2) LS term of the NN effective interaction, 3) $\mu_0 \neq \mu_N$ components. The results, multiplied by the maximum occupation numbers of $0p_{1/2}$ and $0p_{3/2}$ orbitals, are shown in the right panel of Fig. 2. As expected, $A_z(0p_{1/2})$ and $A_z(0p_{3/2})$ show completely opposite behavior, and both are symmetric with respect to $\phi_{12} = 180^\circ$.

4 Discussion and Summary

The observable A_z provides a useful probe of single-particle motion in nuclei. Compared with conventional coplanar observables, it is intrinsically sensitive to three-dimensional non-coplanar geometry and is therefore complementary to transverse analyzing power A_y. The same strategy can be extended to other proton-induced knockout reactions with at least three final-state particles, provided the spin correlation coefficient is sufficiently large. For future measurements, combined analysis of cross sections, A_y, and A_z is expected to improve the extraction of various interaction terms relevant to structure and reaction calculations. The method is also promising for inverse-kinematics experiments on unstable nuclei, where wide azimuthal acceptance and non-coplanar kinematics can be exploited efficiently.

We have introduced a longitudinally polarized proton beam to induce chirality in the $(p, 2p)$ reaction. Under the non-coplanar kinematics in the final state, the longitudinal vector analyzing power A_z can distinguish the orbital motion of the knocked-out proton, whose spin is effectively selected to be parallel to the beam helicity, due to the large spin correlation coefficient C_{zz} of the pp scattering at the intermediate energy.

An intuitive understanding of A_z is introduced, and the theoretical calculation based on the standard DWIA shows the expected behavior of A_z as a function of ϕ_{12}. It is also possible to perform a simplified DWIA calculation incorporating the assumptions in the intuitive picture, and the results agree with the expectations.

Kinematic selection is also important. The calculations indicate that the central non-coplanar region provides a favorable balance between the cross section and A_z. Combined analysis of TDX, A_y, and A_z is expected to give stronger constraints on reaction dynamics and structure than any single observable. For inverse-kinematics experiments on unstable nuclei, the method is expected to be promising. Non-coplanar observables benefit from wide azimuthal coverage, and modern detector systems can sample mirror-partner configurations efficiently. This suggests that chirality-sensitive spin observables may become a useful tool for spectroscopy of exotic systems.

Acknowledgments

We wish to acknowledge T. Uesaka for valuable comments and discussions. This work is supported in part by Grant-in-Aid for Scientific Research (No. JP20K14475, No. JP21H04975, No. JP25K07302, and No. JP25K17400) from Japan Society for the Promotion of Science (JSPS), and JST ERATO Grant No. JPMJER2304, Japan.

References

[1] T. Edagawa, K. Yoshida, S. Kawase, K. Ogata, and M. Sasano, "Chirality in $(\vec{p}, 2p)$ reactions induced by proton helicity", Phys. Rev. C **113**, L031601 (2026).

[2] G. Jacob and T. A. J. Maris, "Quasi-Free Scattering and Nuclear Structure", Rev. Mod. Phys. **38**, 121–142 (1966).

[3] G. Jacob and T. A. J. Maris, "Quasi-Free Scattering and Nuclear Structure. II.", Rev. Mod. Phys. **45**, 6–21 (1973).

[4] T. Wakasa, K. Ogata, and T. Noro, "Proton-induced knockout reactions with polarized and unpolarized beams", Progress in Particle and Nucl. Phys. **96**, 32 (2017).

[5] T. Noro *et al.* "Experimental study of $(p,2p)$ reactions at 392 MeV on ^{12}C, ^{16}O, ^{40}Ca and ^{208}Pb nuclei leading to low-lying states of residual nuclei", Prog. Theor. Exp. Phys. **2020**, 093D02 (2020).

[6] T. Noro *et al.* "Experimental study of $(p, 2p)$ reactions at 197 MeV on ^{12}C, ^{16}O, ^{40,48}Ca, and ^{90}Zr nuclei leading to low-lying states of residual nuclei", Prog. Theor. Exp. Phys. **2023**, 093D01 (2023).

[7] T. J. Maris, M. R. Teodoro, and E. A. Veit, "Effective polarization in quasi-free scattering", Phys. Lett. B **94**, 6–8 (1980).

[8] Shubhchintak, C. A. Bertulani, and T. Aumann, "Maris polarization in neutron-rich nuclei", Phys. Lett. B **778**, 30–34 (2018).

[9] N. S. Chant and P. G. Roos, "Distorted-wave impulse-approximation calculations for quasifree cluster knockout reactions", Phys. Rev. C **15**, 57–68 (1977).

[10] N. S. Chant and P. G. Roos, "Spin orbit effects in quasifree knockout reactions", Phys. Rev. C **27**, 1060–1072 (1983).

[11] K. Ogata, K. Yoshida, and Y. Chazono, "PIKOE: a computer program for distorted-wave impulse approximation calculation for proton induced nucleon knockout reactions", Comput. Phys. Commun. **297**, 109058 (2024).

[12] S. Hama, B. C. Clark, E. D. Cooper, H. S. Sherif, and R. L. Mercer, "Global Dirac optical potentials for elastic proton scattering from heavy nuclei", Phys. Rev. C **41**, 2737–2755 (1990).

[13] E. D. Cooper, S. Hama, B. C. Clark, and R. L. Mercer, "Global Dirac phenomenology for proton-nucleus elastic scattering", Phys. Rev. C **47**, 297–311 (1993).

[14] E. D. Cooper, S. Hama, and B. C. Clark, "Global Dirac optical potential from helium to lead", Phys. Rev. C **80**, 034605 (2009).

[15] W. G. Love and M. A. Franey, "Effective nucleon-nucleon interaction for scattering at intermediate energies", Phys. Rev. C **24**, 1073–1094 (1981).

[16] M. A. Franey and W. G. Love, "Nucleon-nucleon t-matrix interaction for scattering at intermediate energies", Phys. Rev. C **31**, 488–498 (1985).

[17] A. Bohr and B. R. Mottelson, *Nuclear Structure* (W. A. Benjamin, 1969).